
5.1 INTRODUCTION

The Self-Micro Emulsifying Drug Delivery System (SMEDDS) is one of the most widely used systems to overcome solubility and low oral absorption of water-insoluble drugs. SMEDDS contains isotropic mixture of oil, surfactant, and cosurfactant, which form fine oil-in-water (o/w) emulsions upon dilution in aqueous medium and gentle agitation provided in the gastrointestinal tract (1). Spontaneous formation of a microemulsion delivers the drug in a solubilized form; further, small droplet size allows rapid dissolution of the drug and provides a large surface area for its absorption, enhancing its permeation across the intestinal membrane. In addition, the drug solubilized in oil droplets is carried by lymphatic transport through the intestine to avoid first-pass metabolism in the liver (2). Hence, AM loaded SMEDDS (AM-SMEDDS) were formulated to overcome first pass metabolism and improve oral bioavailability of Asenapine maleate.

The D-optimal mixture design, a subtype of mixture design, is one of the most popular response surface methodologies for optimizing formulation of a SMEDDS. The D-optimal mixture design minimizes the variance associated with evaluation of coefficients in a model and produces the best possible subset by considering the criteria for maximizing information matrix determinants. The Central Composite, Box–Behnken, and factorial designs do not consider the total system of SMEDDS formulation, while the D-optimal mixture design considers the total system of SMEDDS as 100% (3).

This design is restricted to $X_1+X_2+\dots+X_n=1$. The regression equation of this design is somewhat different from traditional polynomial equation and is termed as CANONICAL polynomial. Here, AM loaded SMEDDS were prepared and optimized using D-optimal mixture design.

5.2 MATERIALS

Asenapine maleate (AM) was received as a gift sample from Alembic Pharmaceuticals Ltd., Vadodara, India. Peceol, Capryol 90, Lauroglycol 90, Labrasol, Capmul MCM, Labrafil M 1944 CS, Labrafil M 2125 CS, Transcutol HP, Lauroglycol FCC were obtained as gift samples from Gattefosse India Private Limited, Mumbai, India. Capmul MCM C8, Captex 500, Capmul PG8 were obtained from Abitec, USA, Cremophor EL, Cremophor RH40 were obtained as gift samples

from BASF India Ltd., Mumbai, India. All other chemicals and reagents used were of analytical grade.

5.3 PREFORMULATION STUDIES

5.3.1 Solubility of AM in oils, surfactants and co-surfactants

The solubility of AM was determined in various oils (Oleic acid, Capryol 90, Capmul MCM, Capmul MCM C8), surfactants (Ibranol, Tween 80, Tween 20 etc.) and co-surfactants (Transcutol HP, propylene glycol etc.). The solubility was determined by dissolving an excess amount of AM in 2 mL each of the component in 5-mL stoppered vials and mixed using a vortex mixer. The vials were then kept at 37 ± 1.0 °C in an isothermal shaker for 72 hours to get equilibrium. The equilibrated samples were removed from the shaker and centrifuged at 3000 rpm for 15 min. The supernatant was taken and filtered through a 0.45- μ m membrane filter and solubility of AM was subsequently quantified by UV-visible spectrophotometer at 270 nm (4).

5.3.2 Screening of surfactants

Screening of surfactants was carried out using emulsification test. 500 μ l of oil and 500 μ l of surfactant was mixed to form homogenous solution. 100 μ l of oil surfactant mixture was diluted to 50 ml with water and percentage transmittance was measured using UV spectrophotometer at 630 nm (5,6) using distilled water as blank.

5.3.3 Screening of co-surfactants

Screening of co-surfactants was carried out using emulsification test. 500 μ l of surfactant was mixed with 250 μ l of co-surfactant. 500 μ l of oil was mixed with 500 μ l of surfactant-co-surfactant mixture. Then 100 μ l of this mixture was diluted to 50 ml with water and percentage transmittance was measured using UV spectrophotometer at 630 nm using distilled water as blank (5,6).

5.3.4 Construction of pseudoternary phase diagram

Pseudo ternary phase diagram can be represented as a triangle having three coordinates represents one component of microemulsion system viz. oil phase, surfactant/co-surfactant (S_{mix}) phase and aqueous phase. Pseudo ternary phase diagram was constructed to choose appropriate components and their concentration ranges that can result into large microemulsion (7).

In this method, surfactant was blended with co-surfactant in fixed weight ratios (1:0, 1:1, 2:1, 3:1, 1:2 and 1:3 w/w). For each phase diagram, the ratio of oil to the S_{mix} was varied as 1:9, to 9:1 (w/w) to delineate the boundaries of microemulsion region.

The homogenous mixture of oil and Smix was subjected to aqueous titration with the addition of water in each step, and was visually observed. The amount of water at which transparency-to-turbidity transition occurs was derived from the weight measurements. The phase diagram was plotted using CHEMIX ternary plot software (8).

5.4 FORMULATION DEVELOPMENT

AM was added in the oil in small increment with continuous stirring. The surfactant system was prepared by mixing separately the chosen surfactant and cosurfactant in their determined ratios. Oil phase containing AM was added in the surfactant system solution with continuous stirring until a homogenous mixture formed. The resultant AM-SMEDDS formulation was subjected to further characterization (9).

5.5 OPTIMIZATION USING D-OPTIMAL DESIGN

The D-optimal mixture design, a subtype of mixture design, is one of the most popular response surface methodologies for optimizing formulation of a SMEDDS. The factors selected for D-optimal design were Oil concentration, Surfactant concentration and Co-surfactant Concentration (3,10). Coded and actual values are shown in table 5.1. Globule size (Y_1), % transmittance (Y_2) and self-emulsification time (Y_3) were taken as dependent variables.

Table 5.1: The coded and actual values of independent variables for AM-SMEDDS

Factors	Levels		
	-1	0	+1
X ₁ : Oil Concentration (%)	10	20	30
X ₂ : Surfactant Concentration (%)	30	45	60
X ₃ : Co surfactant Concentration (%)	20	30	40

Contour plots and response surface plots aids in understanding of main and interaction effects of independent variables on responses. Contour and response surface plots were generated using design expert software.

5.5.1 Establishment of Design Space

Design space was generated by selecting constraints (minimum particle size, maximum transmittance and minimum self-emulsification time) for the desired

response. The batch suggested by software was prepared using same procedure as described above and predicted value was compared with observed value.

5.5.2 Analysis of design space robustness

Overlay plot was generated using design expert to evaluate robustness of established design space with selecting response to higher and lower value of established design space. The software suggested values for independent variables in and around established design space along with value of the desired responses.

5.5.3 Statistical analysis

The results were presented as mean \pm standard error of the mean. The experimental data were validated by ANOVA, regression coefficient, lack of fit test and $p < 0.05$ was considered as significant.

5.6 CHARACTERIZATION

5.6.1 Globule size and Zeta potential determination

1 ml of the formulation was diluted to 100 times with purified water and was employed to determine the globule size and zeta potential using zetasizer (Malvern Instruments, Malvern, UK).

5.5.2 Robustness to dilution

Robustness of SMEDDS to dilution was studied by diluting it 50,100 and 1000 times with various dissolution media i.e. water, gastric fluid pH 1.2 and phosphate buffer pH 6.8. The diluted samples were stored for 24 h and observed for any signs of phase separation or precipitation (11).

5.6.3 Determination of self-emulsification time

The emulsification time of SMEDDS formulations was determined using USP type II (paddle type) dissolution apparatus. 1 ml of formulation was added to 500 ml purified water at 37 °C. Gentle agitation was provided by a standard stainless-steel dissolution paddle rotating at 50 rpm. The time required to obtain clear dispersion was recorded as emulsification time. The self-emulsification capability of formulation was evaluated on the basis of following grades shown in table 5.2 (8).

Table 5.2: Classification of the SMEDDS Formulation in Accordance to Comparative Grades

Grade	Dispersibility and appearance	Time of self-emulsification (min)
I	Rapid forming microemulsion, which is clear or slightly bluish in appearance	<1
II	Rapid forming, slight less clear emulsion, which has a bluish white appearance	<2
III	Bright white emulsion (similar to milk in appearance)	<2
IV	Dull, grayish white emulsion with a slight oily appearance that is slow to emulsify	>3
V	Exhibit poor or minimal emulsification with large oils droplets present on the surface	>3

5.6.4 Cloud point measurement

The cloud point is a crucial factor for SMEDDS containing non-ionic surfactants. 1 ml formulation was diluted 250 times with distilled water, placed in a water bath and temperature was gradually increased. The point at which cloudiness appeared was noted as cloud point (12).

5.6.5 Drug content estimation

1 ml of SMEDDS was dissolved in 10 ml of methanol. The solution was filtered through 0.45 μ membrane filter (Millipore, Mumbai, India), suitably diluted and analyzed using UV-VIS spectrophotometer (UV 1800, Shimadzu AS, Japan) at 270 nm.

5.6.6 Viscosity determination

The viscosity of the prepared SMEDDS formulations was determined as such without dilution by Rheometer (Cone and Plate DV III, Brookfield Engineering Laboratories, Inc., MA, USA) (13,14).

5.6.7 Percentage Transmittance

A total of 1 mL of SMEDDS formulation was diluted 100 times with deionized water. Percentage transmittance was measured spectrophotometrically at 630 nm using deionized water as a blank.

5.6.8 Thermodynamic stability

The optimized batch of SMEDDS (diluted 100 times with distilled water) was subjected to different thermodynamic stability tests in order to assess their physical stability. All samples were evaluated in terms of phase separation at the end of analysis (15).

Heating–cooling cycle. Six cycles between refrigerator temperature (2–8 °C) and 45°C with storage at each temperature not less than 48 h were conducted.

Centrifugation test. Each of formulation was centrifuged at 12,000 rpm for a period of 10 min.

5.6.9 Fourier transform infrared spectroscopy (FTIR)

The IR spectra of AM, Capryol 90, physical mixture of AM and excipients and AM-SMEDDS were recorded on Fourier Transform Infra-red spectrophotometer (Shimadzu, Japan).

5.6.10 Transmission Electron Microscopy (TEM)

20 µl of sample was taken on carbon film coated on copper grid and allowed to air dry. Then it was treated with phosphotungstic acid for negative staining. After 5min, the grid was placed in the sample probe inserted in Transmission Electron Microscope (Philips, Tecnai 20, Holland) and observed at 200 kV accelerating voltage.

5.7 IN VITRO DRUG RELEASE STUDY

The in vitro release studies of SMEDDS were carried out in gastric fluid pH 1.2 and phosphate buffer pH 6.8 using dialysis bags with a molecular cut off 12000-14000 Da. AM-SMEDDS and AM suspension equivalent to 10 mg was placed in the dialysis bag, clamped at both ends and introduced into a 250 mL of release medium. The entire system was kept under magnetic stirring at 100 rpm/min at 37±1°C and covered to prevent water evaporation. At predetermined time intervals, the aliquots were withdrawn and replaced with fresh diffusion medium. The samples were filtered and drug concentration was determined using UV spectroscopy at 270 nm (11).

5.8 EX VIVO PERMEABILITY STUDY

Ex vivo permeability studies of SMEDDS drug suspension were performed to determine transport of AM through biological membrane. The studies were carried out using Sprague–Dawley rat's stomach and intestine. The protocol was approved by the Institutional Animal Ethics Committee of M.S. University of Baroda, Vadodara, India (MSU/IAEC/2017-18/1643). Rats (250-300g) were sacrificed by euthanasia and

part of stomach and intestine was immediately removed, thoroughly washed and placed in phosphate buffer pH 7.4. A volume equivalent to 10 mg AM each of Am-SMEDDS and AM-suspension were added in lumen of stomach and tied at each end with a thread. Then the tissue was placed in an organ tube containing 30 ml of phosphate buffer pH 7.4 with continuous aeration, the temperature was maintained 37 ± 1 °C. At predetermined time intervals (0.5, 1 and 2 h), samples were withdrawn and replenished by the same volume of fresh buffer solution. After 2 h, the contents of stomach were transferred into the lumen of intestine and tied at each end with a thread (1,2). At predetermined intervals of time (4, 6, 8 and 10 h), aliquots were withdrawn from the receptor compartment, filtered through 0.22 μ membrane filter and analyzed by UV spectrophotometer (UV 1800, Shimadzu AS, Japan) at 269 nm (16,17).

5.9 STABILITY STUDY

The optimized batch was subjected to stability studies, carried out at 30 ± 2 °C/60% \pm 5% RH. The formulation was kept in air-tight glass vials and assayed periodically, at the time points of 0, 1, 2 and 3 months, for drug content, globule size, zeta potential and self-emulsification time (4).

5.10 RESULTS AND DISCUSSION

5.10.1 PREFORMULATION STUDIES

5.10.1.1 Solubility of AM in oils, surfactants and co-surfactants

The AM-SMEDDS were prepared to increase solubility and bioavailability of drug via oral route. Thus, the oil was selected in such a way that it had maximum solubilizing capacity for AM (18).

The solubility of drug in excipients plays an important role in determining stability of formulation, as many formulations undergo precipitation before undergoing in situ solubilization (18). Oil can solubilize marked amounts of lipophilic drug and can increase the fraction of lipophilic drug transported via the intestinal lymphatic system, thereby increasing absorption from the GIT depending on the molecular nature of the triglycerides (19). Solubility of drug in oil phase is crucial for the development of SMEDDS as it determines drug loading efficiency and soluble portion of drug during storage and in vivo dilution. There could be a risk of drug precipitation from SMEDDS during dilution in GIT due to lowering of solvent capacity if surfactant or co-surfactant contributes to drug solubilization (20,21). Hence, to formulate robust SMEDDS, oil with best solubilizing capacity should be selected.

Amongst the various oils screened (Figure 5.1), the maximum saturated solubility of AM was obtained in Capryol 90 having HLB 5. This was advantageous as it has unsaturated fatty acids in its structure which more effectively supports lymphatic drug transport than saturated orally administered fatty acids (22).

The maximum solubilizing capacity of AM in Capryol 90 may have arisen from the higher ester bond content per gram of the medium chain glycerides. Therefore, in order to achieve ideal drug loading and to avoid precipitation of the drug on dilution in the gut lumen in vivo, Capryol 90 was selected for further study as oil phase for formulation development (23,24).

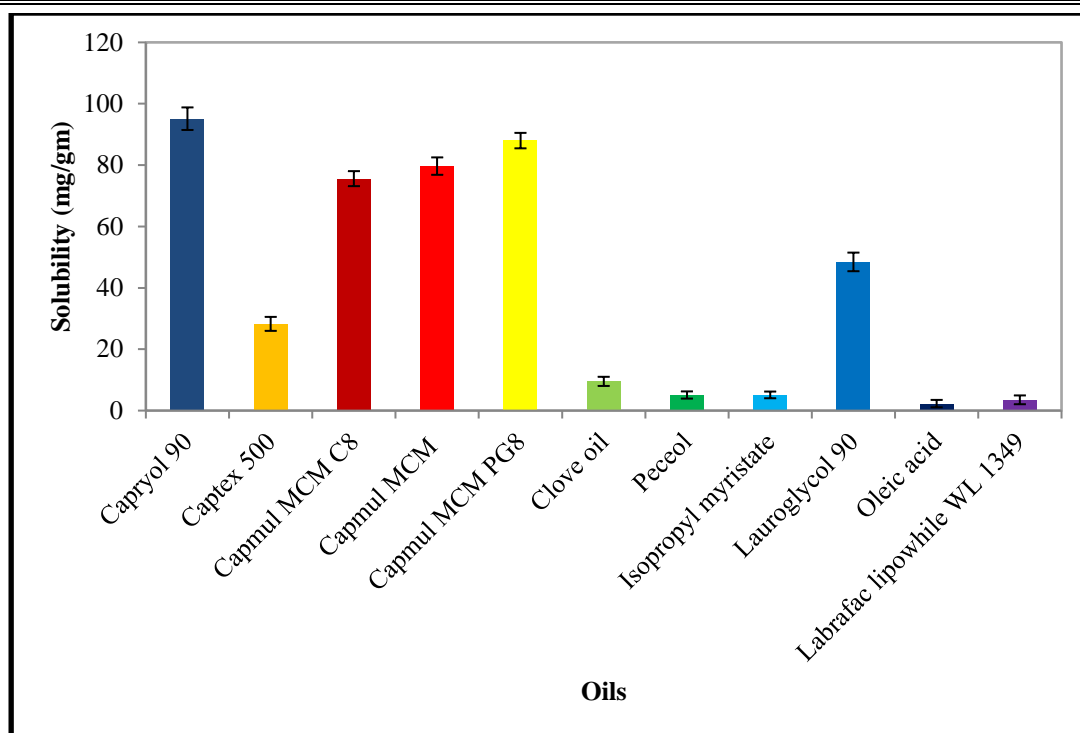


Figure 5.1: Solubility of Asenapine maleate in various oils

When the solubility of AM was studied in different surfactants and co-surfactants (Figure 5.2 & 5.3), maximum solubility of drug was observed in Labrasol and Transcutol HP respectively.

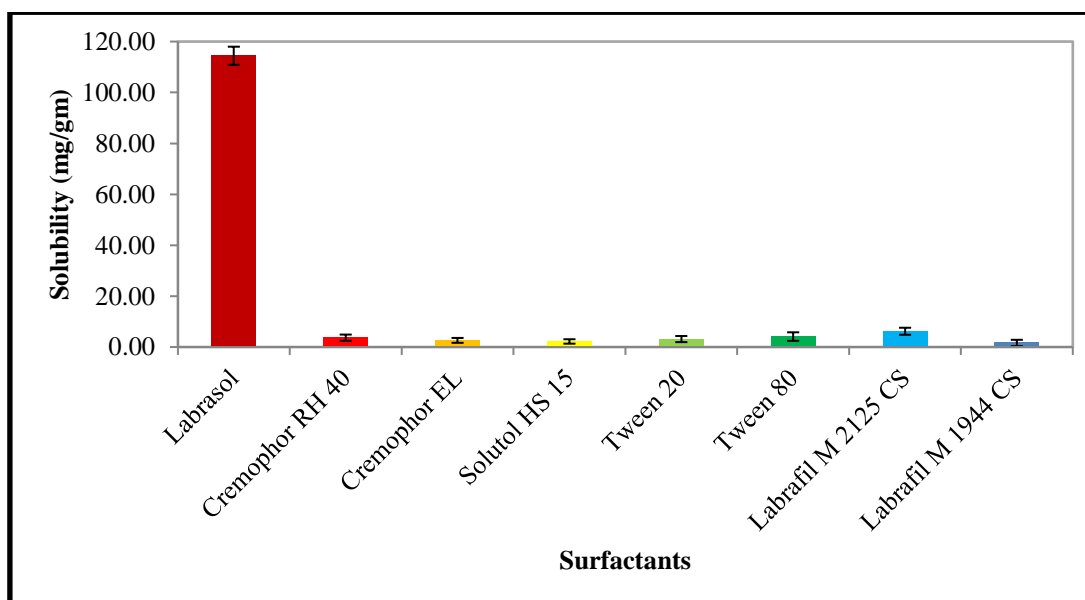


Figure 5.2: Solubility of Asenapine maleate in various surfactants

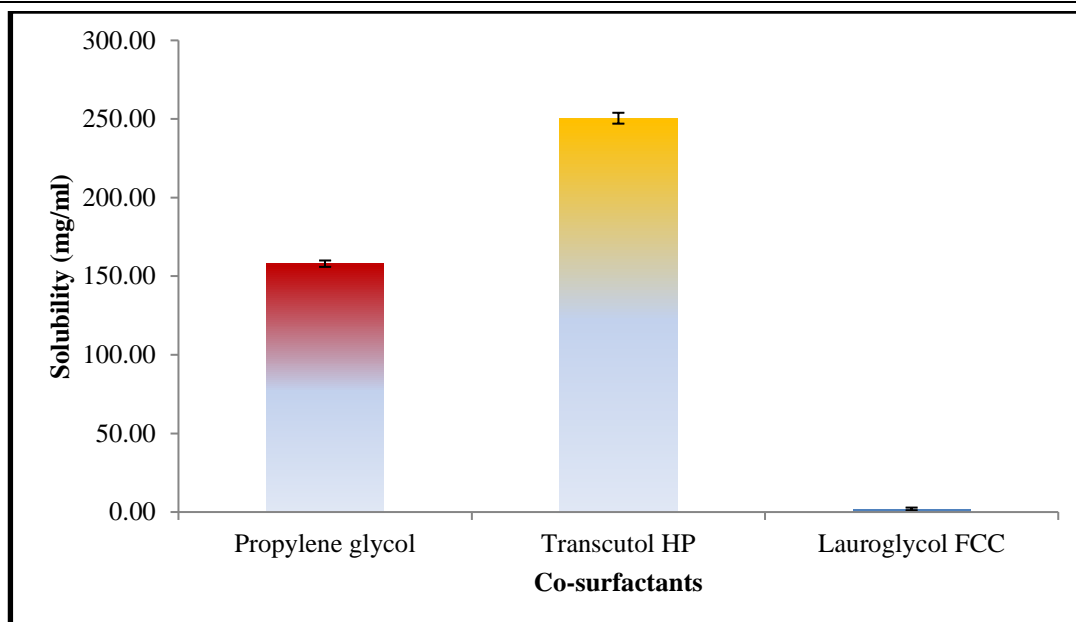


Figure 5.3: Solubility of Asenapine maleate in various co-surfactants

5.10.1.2 Screening of surfactant

Addition of surfactant is necessary because it adsorbs around oil–water interface and decreases the emulsion droplet size owing to decreased interfacial tension of the system (25). Moreover, decrease in droplet size indicates close packed arrangement of surfactant at the oil–water interface and improved stabilizing effect on oil droplets by forming a strong mechanical barrier to coalescence (20).

The surfactants exert their absorption enhancing effect by partitioning into the cell membrane to disrupt the structural organization of the lipid bilayer leading to permeation enhancement (26).

Nonionic surfactants were screened for fabrication of SMEDDS as they are less toxic, typically have lower critical micelle concentration and are accepted for oral ingestion as compared to their ionic counterparts (20,23). In addition, they can produce reversible changes in intestinal mucosa, thus leading to enhanced permeability and absorption of drug (27).

A right combination of low (hydrophobic) and high HLB (hydrophilic) surfactant is essential for the formation of a stable nanoemulsion, in the development of a self-emulsifying formulation (23).

It has been reported that well formulated SMEDDS is dispersed within seconds under gentle stirring conditions (28). Transmittance values of different mixtures are demonstrated in figure 5.4. Emulsification study clearly distinguished the ability of surfactants to emulsify oil. Cremophor EL (polyoxy 35 castor oil, HLB 12-14) had

highest ability to emulsify oil (Capryol 90) as compared to other surfactants. It was also reported that Cremophor EL has bioactive property such as inhibitory effect on P-gp and CYP 450 enzymes (22). So, inspite of highest solubility of drug in Labrasol, Cremophor EL was selected as surfactant owing to its emulsifying ability and bioactive property.

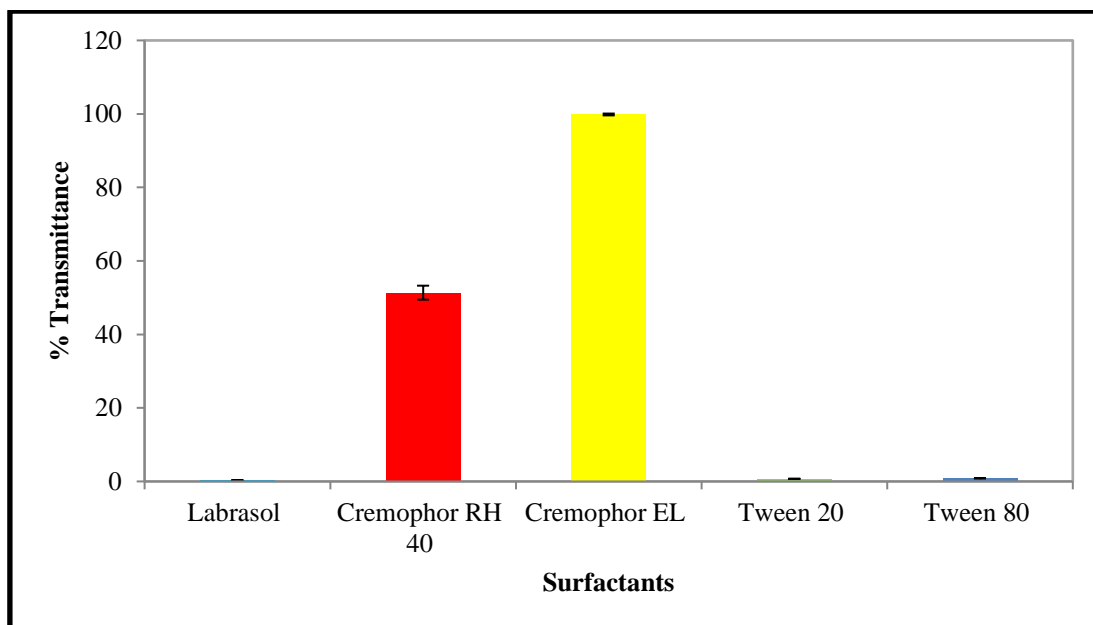


Figure 5.4: Emulsification study of Asenapine maleate in surfactants

5.10.1.3 Screening of Co- surfactant

The thermodynamic stability of SMEDDS can be improved by addition of co-surfactant which may help in reducing interfacial energy and formation of mechanical barrier to coalescence (18). Incorporation of a co-surfactant in the formulation containing surfactant was also reported to improve dispersibility and drug absorption from the formulation (23).

The co-surfactant penetrates into the interface causing void spaces for water penetration. This increases interfacial fluidity that facilitates spontaneous formation of emulsion (27). In the current investigation, three different co-surfactants were tried and Transcutol HP (HLB 4) showed good emulsification ability with highest transmittance (Figure 5.5). Co-surfactant (Transcutol HP) with a shorter molecular chain length (C_6) is considered to be more efficient and has better ability to promote water penetration.

Generally, the longer the length of the hydrophobic alkyl chain, the higher will be the molecular volume of the oil phase affecting the emulsification ability of surfactant

mixtures. Capryol 90 in this context is a C8 medium chain fatty acid of mono- and diester of caprylic acid that can be emulsified with ease (18,29).

The incorporation of suitable co-surfactant lowers the interfacial tension, fluidizes the hydrocarbon region of the interfacial film, and decreases the bending stress of the interface, resulting in the improvement in spontaneity of emulsification, reduction in emulsion droplet size and polydispersity (20).

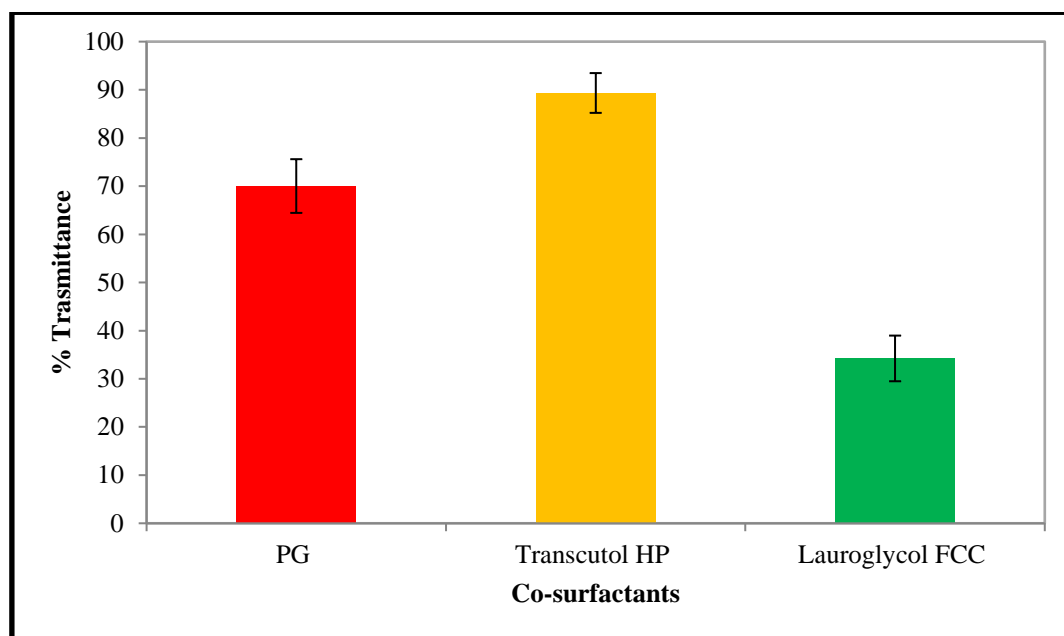


Figure 5.5: Emulsification study of Asenapine maleate in co-surfactants

5.10.1.4 Construction of pseudo ternary phase diagram

A ternary phase diagram was constructed to determine the self-microemulsifying region and to quantify the probable concentration of oil, surfactant and co-surfactant to develop a stable SMEDDS. Drawing of ternary phase diagrams gives an idea about composition and the nature of the resultant dispersions such as phase separation, coarse emulsions, self-nanoemulsification, and, hence, assists in selecting optimum formulation (18,20).

It has been reported that in self-emulsifying system a liquid crystalline phase forms between the oil/surfactant and water phases which effectively swells and facilitates spontaneous formation of an interface between the oil droplets and the water (20). For the system to be self-emulsifying, surfactants used should be able to increase dispersion entropy, reduce the interfacial tension, increase interfacial area and lower the free energy to a minimum (18,19).

Ternary diagrams in six different weight ratios of surfactant to co-surfactant (S/Cos) were plotted between Capryol 90, Cremophor RH 40 and Transcutol HP as oil,

surfactant and co-surfactant phase respectively (Figure 5.6). It was observed that at 1:0 ratio of S/Cos, smaller microemulsion region was observed as only surfactant was not be able to reduce o/w interfacial tension sufficiently. The maximum region was observed at 1:1 ratio of S/Cos. Further increase in surfactant from 1:1 to 1:3 showed decrease in formation of nanoemulsion region indicating optimum emulsification was achieved at 1:1 ratio of S/Cos. Increase in co surfactant concentration also decreased microemulsion region as excessive amount of co-surfactant will cause the system to become less stable due to its intrinsic high aqueous solubility and lead to increase in the droplet size as a result of the expanding interfacial film. Hence, 1:1 ratio was considered as optimum surfactant:co-surfactant ratio.

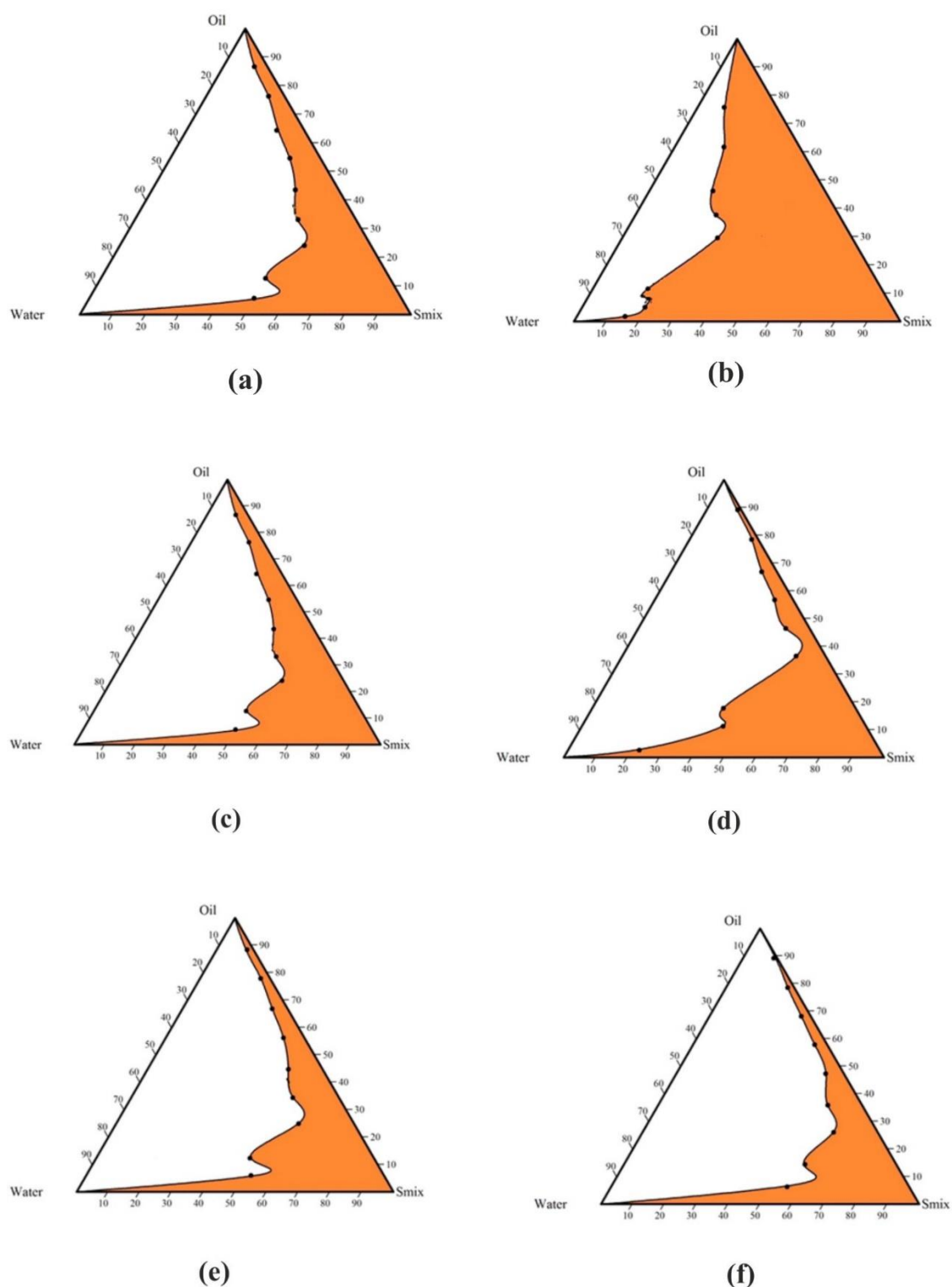


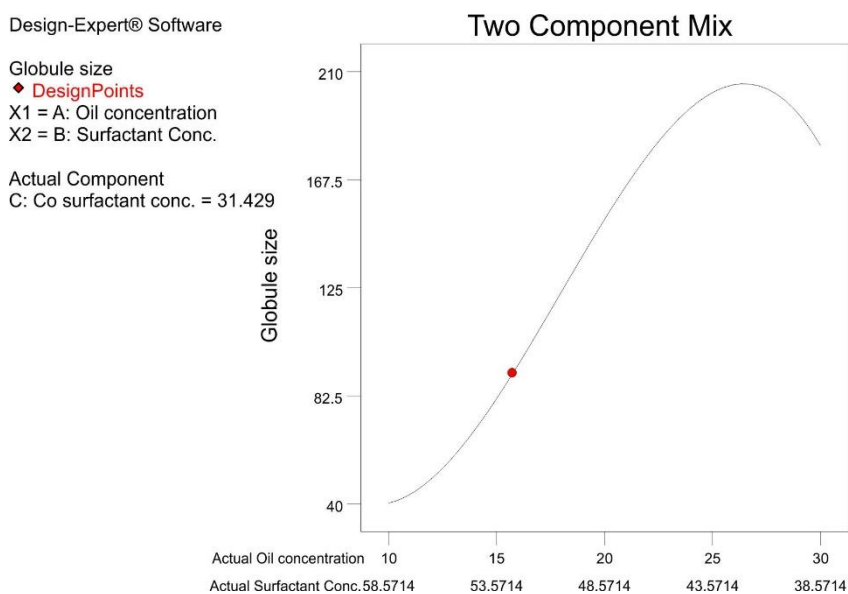
Figure 5.6: Ternary diagrams of Capryol 90 with different ratio of Cremophor EL and Transcutol HP (a)1:0, (b)1:1, (c)2:1, (d)3:1, (e)1:2 and (f)1:3

Table 5.4: ANOVA analysis for globule size of AM-SMEDDS

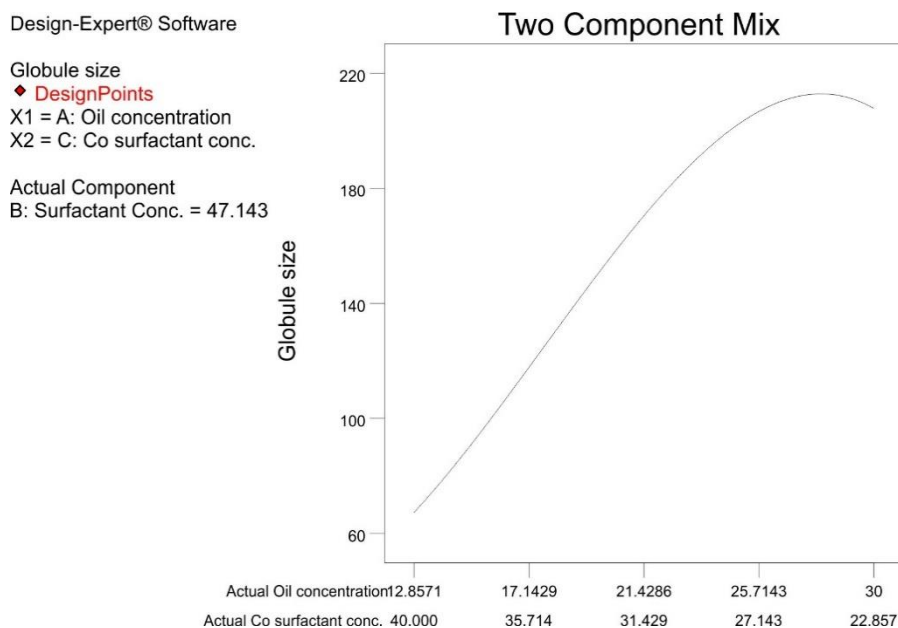
Source	Sum of Squares	df	Mean square	F Value	p-value prob>F
Model	56874.18	9	6319.35	149.87	0.0001
Linear Mixture	49335.53	2	24667.76	585.02	< 0.0001
X ₁ X ₂	1.28	1	1.28	0.030	0.8700
X ₁ X ₃	26.75	1	26.75	0.63	0.4704
X ₂ X ₃	88.07	1	88.07	2.09	0.2219
X ₁ X ₂ X ₃	0.10	1	0.10	2.399E-003	0.9633
X ₁ X ₂ (X ₁ -X ₂)	922.81	1	922.81	21.89	0.0095
X ₁ X ₃ (X ₁ -X ₃)	216.56	1	216.56	5.14	0.0861
X ₂ X ₃ (X ₂ -X ₃)	361.64	1	361.64	8.58	0.0429
Residual	168.66	4	42.17		
Lack of Fit	1.54	1	1.54	0.028	0.8786
Pure Error	167.13	3	55.71		
Cor Total	57042.85	13			

From the results of ANOVA, it was observed that X₁X₂(X₁-X₂) and X₂X₃(X₂-X₃) had significant effect on globule size (p<0.05). Two component mixture plot was generated while keeping the third variable constant to evaluate effect of varying ratio of two variables on the response. Globule size was found to be increased from 40 to 200 nm as X₁ increased and simultaneously X₂ decreased (Figure 5.7a). From the ANOVA results, it was confirmed that X₂ significantly interacted with X₁ (p<0.0095). Increase in Capryol 90, a hydrophobic MCT increases surface tension at the oil water interface that proceeds through a liquid crystalline phase leading to coarser and aggregated droplets (26). Increase in X₂ and decrease in X₁ led to decreased globule size. This might be because the surfactant concentration was enough to reduce interfacial free energy at oil-water interface which prevented coalescence of droplets and reduced globule size. Moreover, decrease in globule size indicated closely packed arrangement of surfactant at oil-water interface and improved stabilization of oil droplets (14,20). Globule size was increased as X₁ increased and X₃ decreased as in case of X₁ and X₂ (Figure 5.7b). X₂ and X₃ ratio also had significant effect on globule size (p<0.0429). It was observed that globule size was increased as X₂ decreased and

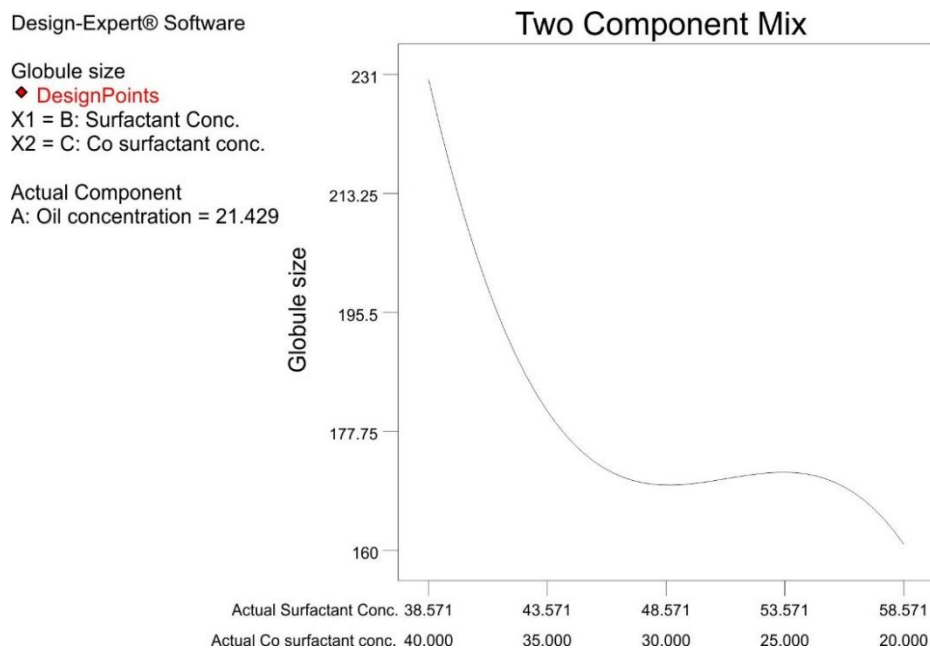
X₃ increased ((Figure 5.7c). This might be because co-surfactant increased the interfacial fluidity by penetrating the surfactant film and consequently creating a disordered film due to the void space among surfactant molecules. This led to enhanced water penetration into oil droplets leading to ejection of oil droplets into aqueous phase which in turn formed coarse emulsion having larger globule size (9,14,26). The combined effect of the independent factors on the globule size was elucidated using contour plot and response surface plot (Figure 5.8).



(a)



(b)



(C)

Figure 5.7: Two-component mixture plot for the effect of varying ratio of two components with a fixed amount of the other component for globule size of AM-SMEDDS

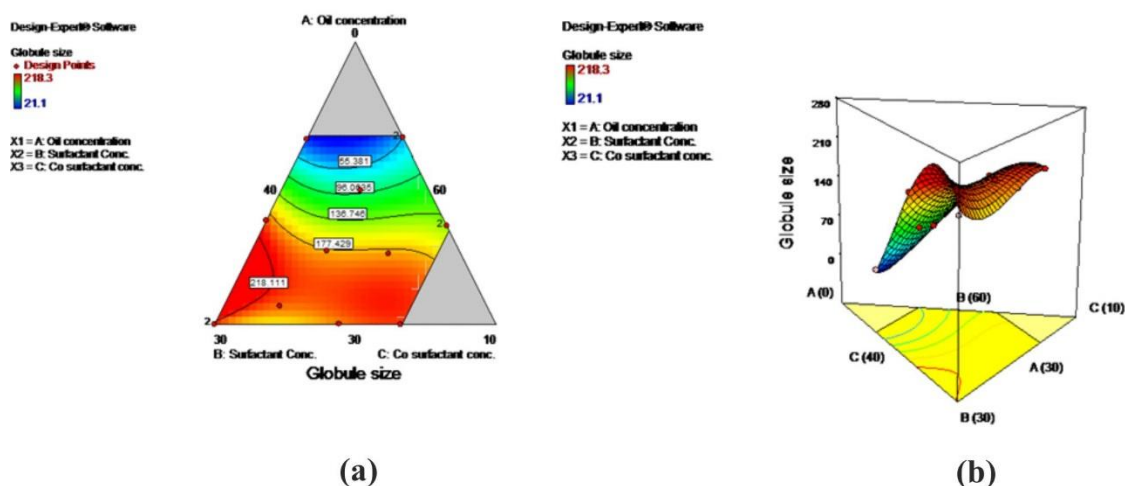


Figure 5.8 : (a) Contour and (b) Response surface plot showing effect of independent variables on globule size of AM-SMEDDS

increased and X_3 decreased, the %transmittance was increased (Figure 5.9c). From these results, it can be clearly observed that the effects of factors upon percentage transmittance were very similar to the effects as observed upon the droplet size but in an opposite direction. Therefore, with increase of oil proportion there was a decrease in clarity of emulsion. This may be attributed to increased interfacial tension between oil and aqueous phase due to insufficient concentration of surfactant system (32). This effect of the independent factors on the %transmittance was further confirmed using contour plot and response surface plot (Figure 5.10).

Design-Expert® Software

Transmittance

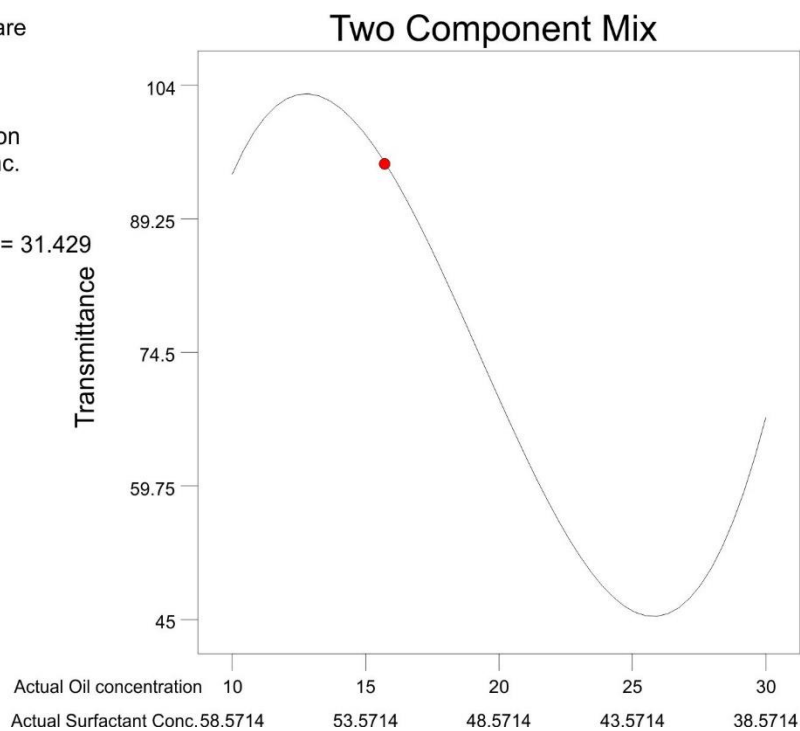
◆ DesignPoints

X1 = A: Oil concentration

X2 = B: Surfactant Conc.

Actual Component

C: Co surfactant conc. = 31.429



(a)

Design-Expert® Software

Transmittance

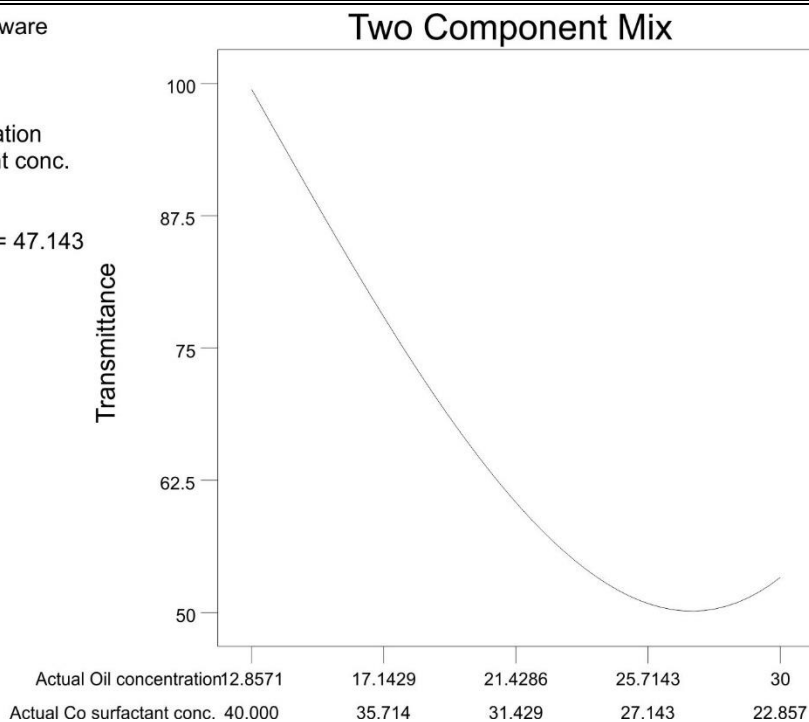
◆ DesignPoints

X1 = A: Oil concentration

X2 = C: Co surfactant conc.

Actual Component

B: Surfactant Conc. = 47.143



(b)

Design-Expert® Software

Transmittance

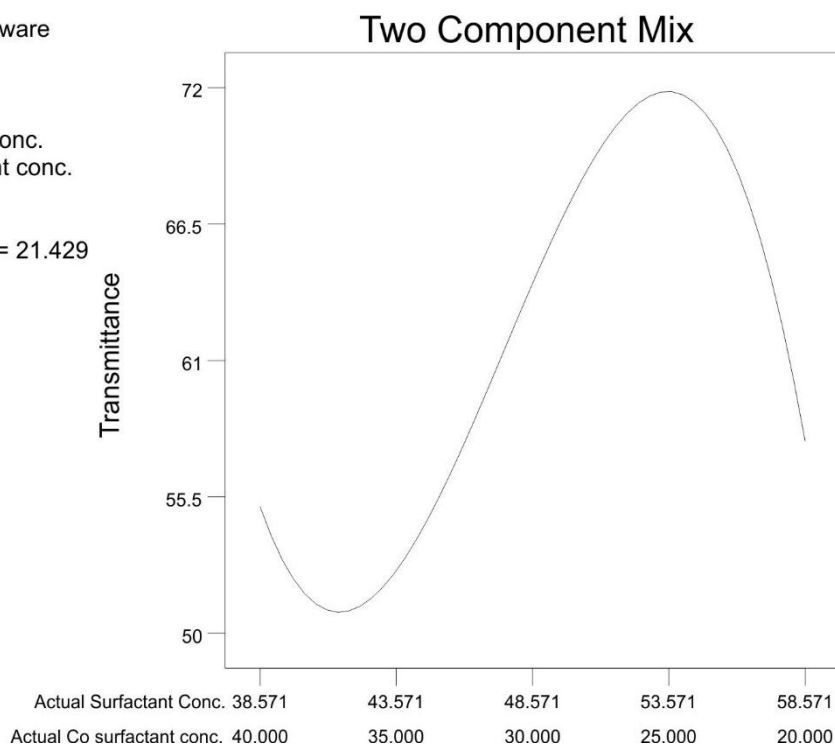
◆ DesignPoints

X1 = B: Surfactant Conc.

X2 = C: Co surfactant conc.

Actual Component

A: Oil concentration = 21.429



(c)

Figure 5.9 : Two-component mixture plot for the effect of varying ratio of two components with a fixed amount of the other component for % transmittance of AM-SMEDDS

Table 5.6: ANOVA analysis for self-emulsification time of AM-SMEDDS

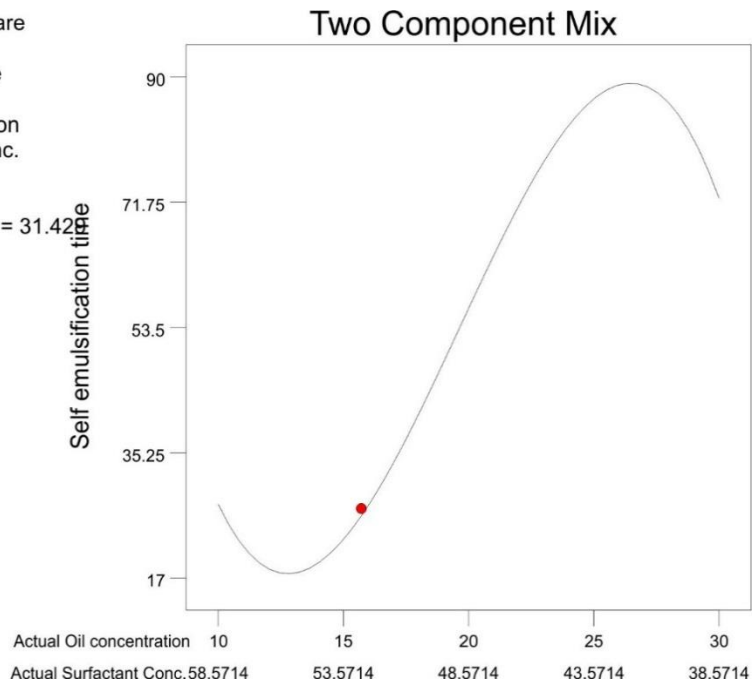
Source	Sum of Squares	df	Mean square	F Value	p-value prob>F
Model	10264.68	9	1140.52	17.25	0.0074
Linear Mixture	5921.58	2	2960.79	44.77	0.0018
X ₁ X ₂	402.60	1	402.60	6.09	0.0691
X ₁ X ₃	1651.54	1	1651.54	24.97	0.0075
X ₂ X ₃	1135.09	1	1135.09	17.16	0.0143
X ₁ X ₂ X ₃	1278.23	1	1278.23	19.33	0.0117
X ₁ X ₂ (X ₁ -X ₂)	645.47	1	645.47	9.76	0.0354
X ₁ X ₃ (X ₁ -X ₃)	47.20	1	47.20	0.71	0.4458
X ₂ X ₃ (X ₂ -X ₃)	1233.97	1	1233.97	18.66	0.0125
Residual	264.53	4	66.13		
Lack of Fit	0.0034	1	0.034	3.818E-004	0.9856
Pure Error	264.50	3	88.17		
Cor Total	10529.21	13			

Two component mixture plot for X₁ and X₂ showed that as X₁ increased and X₂ decreased, the self-emulsification time was found to be increased from 17 to 80 sec (Figure 5.11a). This indicates that X₂ had significantly interacted with X₁. With increase of oil proportion there was an increase in droplet size and that may hinder rate of emulsification which was confirmed by higher emulsification time of the formulations with higher oil concentrations. As X₂ increased and X₁ decreased, self-emulsification time decreased. This could be attributed to reduction in interfacial tension as surfactant arrange themselves at oil-water interface thus leading to increased emulsifying spontenity (33). In case of X₁ and X₃, as X₁ increased and X₃ decreased, self-emulsification time increased ((Figure 5.11b). Two component mixture plot for X₂ and X₃ indicated that increase in X₂ and decrease in X₃ reduced self-emulsification time upto 53% and 25% surfactant and co-surfactant concentration respectively ((Figure 5.11c). Further increase in X₂ to 58% and decrease in X₃ to 20% increased self-emulsificaton time. The reason may be that higher surfactant/oil ratio results in more rapid maturation of the droplets (34). This effect of the independent factors on the self-emulsification time was further confirmed using contour plot and response surface plot (Figure 5.12).

Design-Expert® Software

Self emulsification time
 ◆ DesignPoints
 X1 = A: Oil concentration
 X2 = B: Surfactant Conc.

Actual Component
 C: Co surfactant conc. = 31.42

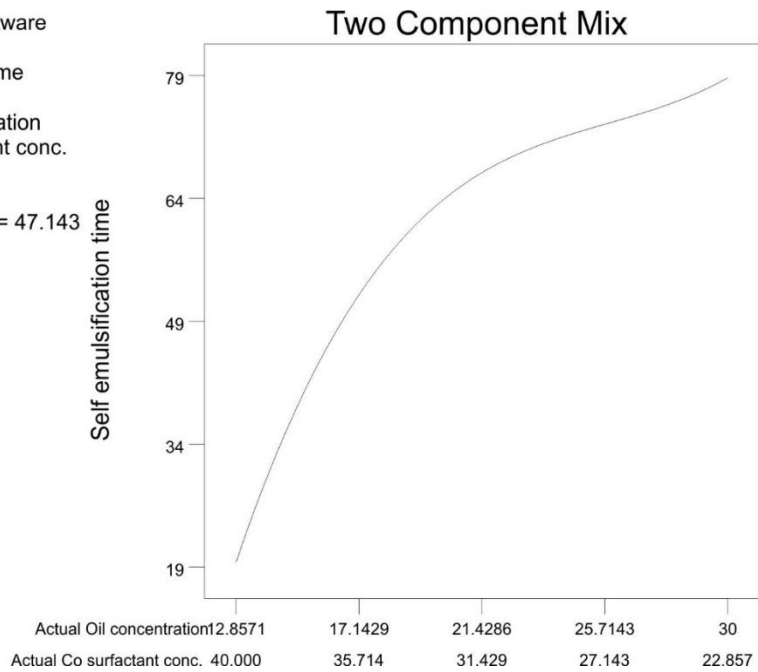


(a)

Design-Expert® Software

Self emulsification time
 ◆ DesignPoints
 X1 = A: Oil concentration
 X2 = C: Co surfactant conc.

Actual Component
 B: Surfactant Conc. = 47.143

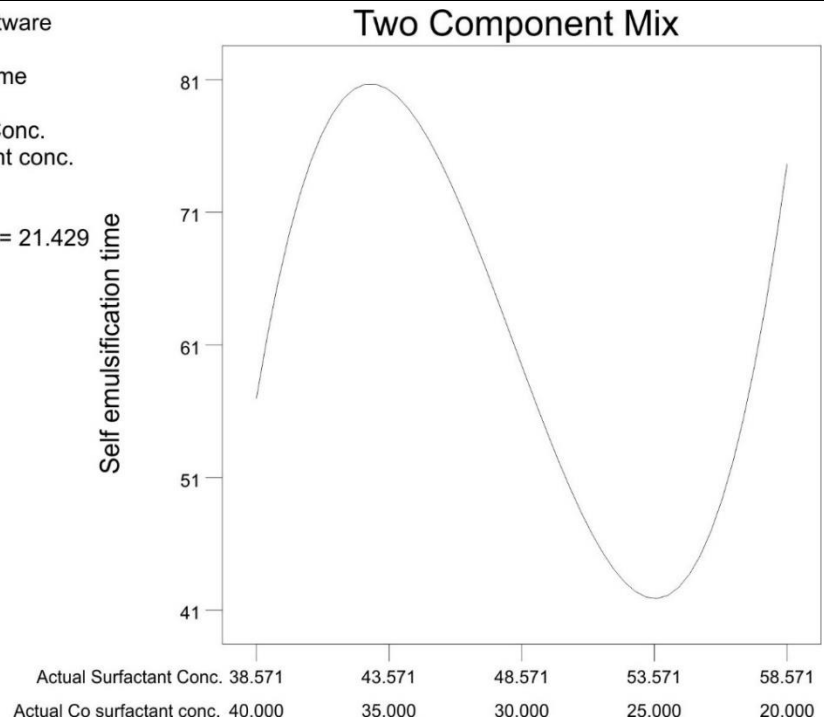


(b)

Design-Expert® Software

Self emulsification time
 ♦ DesignPoints
 X1 = B: Surfactant Conc.
 X2 = C: Co surfactant conc.

Actual Component
 A: Oil concentration = 21.429



(C)

Figure 5.11 : Two-component mixture plot for the effect of varying ratio of two components with a fixed amount of the other component for self-emulsification time of AM-SMEDDS

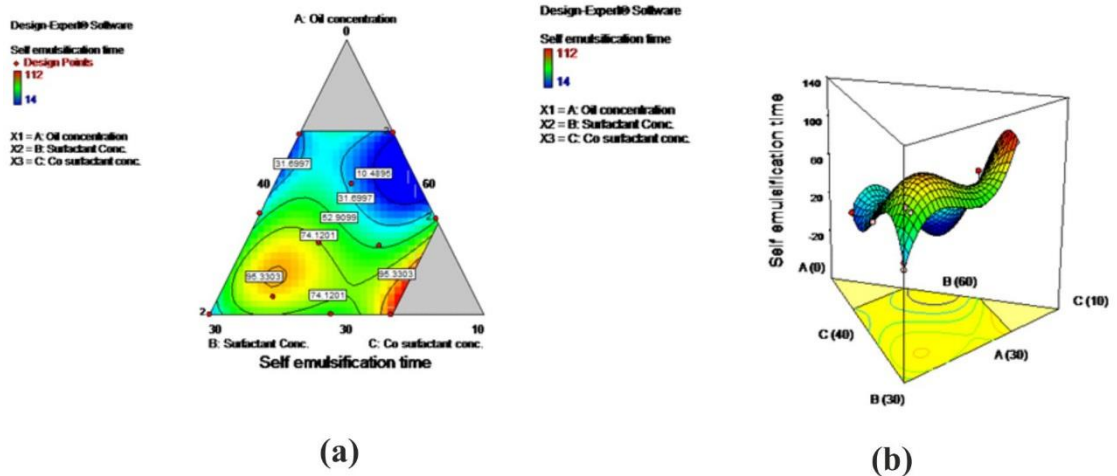


Figure 5.12: (a) Contour and (b) Response surface plot showing effect of independent variables on self-emulsification time of AM-SMEDDS

5.10.2.4 Statistical analysis of designed experiment

The adequacy of the cubic model was verified by ANOVA, lack of fit and multiple correlation coefficient (R^2) tests provided by Design- Expert software. The results of ANOVA showed that p value for response globule size, % transmittance and self-emulsification time was found to be 0.0001, 0.0129 and 0.0074 respectively, for cubic model. Thus it can be concluded that all the responses fitted the model well ($p < 0.05$). Moreover, the lack of fit test is another good statistical parameter for checking the fitness of the model. It compares the residual error with the pure error from the replicated design points. A model with a significant lack-of-fit (Prob>F value 0.10) lacks prediction efficiency, so a non-significant lack of- fit value in the model is highly desirable. The lack of fit value for globule size, % transmittance and self-emulsification time was found to be 0.8786, 0.9166 and 0.9856 respectively. All of these responses fitted in the cubic model showed a non-significant lack-of-fit ($p > 0.1$), proving the adequacy of the model fit (35). Furthermore, the multiple regression analysis for the cubic model is shown as R^2 value, which signifies the measure of the amount of variation around the mean explained by the model. In our study, the R^2 values for the responses globule size, %transmittance and self-emulsification time were 0.9970, 0.9664 and 0.9749 respectively (table 5.7).

Adjusted R^2 on the other hand, provides an estimate of amount of variation about the mean explained by the model, adjusted for specific number of parameters. Predicted R^2 represents the amount of variation in new data explained or predicted by the mathematical model. The closeness of predicted R^2 with R^2 and adjusted R^2 indicates goodness of fit to the data.

The term “Adequate precision” represents signal to noise ratio, and a value of more than 4 is desirable. The high value of adequate precision depicts adequate model discrimination, in other words, adequacy of the signal. The results indicated that all the responses were affected with variations in the studied mixture components.

Table 5.7: Regression analysis for all responses of AM-SMEDDS

	Y_1	Y_2	Y_3
R^2	0.9970	0.9664	0.9749
Adjusted R^2	0.9904	0.8908	0.9183
Predicted R^2	0.9410	0.6138	0.8952
Adeq precision	34.390	10.944	14.042

5.10.2.5 Validation of design

The validation of selected model was carried out using desirability function. The desirability function is a technique used to multi response optimization for the analysis of experiments, in which, several responses have to be optimized simultaneously (36). Check point batch was prepared as suggested by software by selecting constraints for globule size, % transmittance and self-emulsification time to be minimized, maximized and minimized respectively. The predicted and experimental value for the responses are shown in table 5.8. The experimental value for all three responses were found to be in close agreement with predicted value.

Table 5.8: Predicted and observed responses for check point batch of AM-SMEDDS

Response	Predicted value	Experimental value	Percentage prediction error
Y ₁ (nm)	21.10	21.12±1.09	0.09469
Y ₂ (%)	99.22	99.20±0.21	-0.02016
Y ₃ (sec)	28.01	28.0±1.1	0.03571

The desirability of 0.950 for the selected model was obtained (Figure 5.13) indicating the reliability of model for optimization of minimum globule size, maximum % transmittance and minimum self-emulsification time for asenapine maleate loaded SMEDDS.

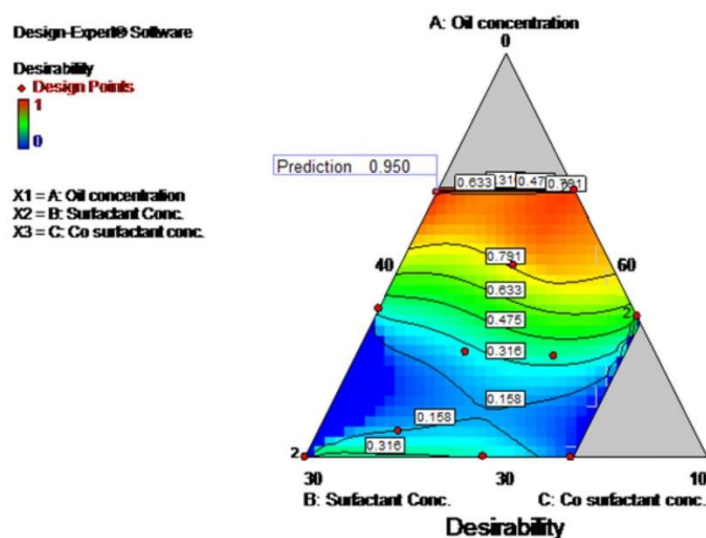


Figure 5.13: Desirability plot of optimized batch of AM-SMEDDS

5.10.2.6 Analysis of Design Space robustness

The design space was earmarked using the aforementioned criteria by a graphical-optimization technique. Figure 5.14 portrays the optimal design space region within the requisite knowledge space and location of the optimum formulation within the desired limits (37). It was observed that value of independent variables outside the design space showed variation in response (Table 5.9). So, it proved that the design space was sensitive to variation in independent variables. The yellow area showed desired response proving the robustness of design space.

Table 5.9: Evaluation of sensitivity of obtained design space of AM-SMEDDS

X ₁	X ₂	X ₃	Y ₁ (nm)		Y ₂ (%)		Y ₃ (sec)	
			Predicted	Observed	Predicted	Observed	Predicted	Observed
10.33	49.66	40.00	18.06	20.1±3.2	98.53	97.6±3.54	29.73	32.0±1.0
17.46	49.74	32.80	115.56	118.7±5.8	82.19	82.0±4.21	44.71	52.0±1.9

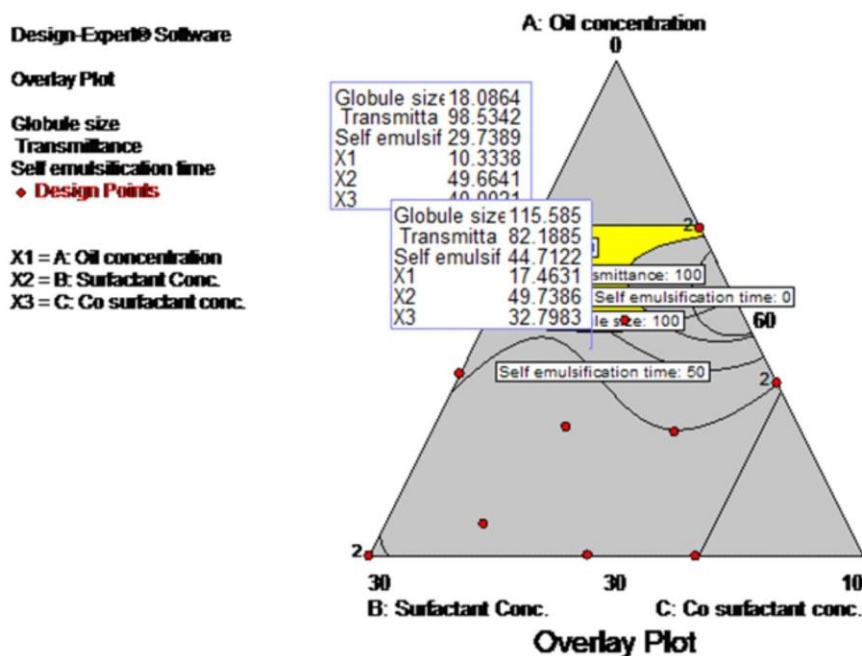


Figure 5.14 Overlay plot depicting the design space of AM-SMEDDS

5.11 CHARACTERIZATION

5.11.1 Globule size determination

The globule size of SMEDDS is a pivotal factor in its self-emulsification performance as it has effect on the rate and extent of drug absorption and release (38). The globule size of the optimized batch was found to be 21.12 ± 1.2 nm with PDI value of 0.144 ± 0.015 indicating unimodal globule distribution (Figure 5.15). The small droplet size indicated adequate surfactant concentration for formation of closed packed film of surfactant at the interface, thereby stabilizing the dispersed droplets (33). This small globule size will provide very high surface area which will aid in absorption of drug and enhance its bioavailability.

Results

	Size (d.nm):	% Intensity	Width (d.nm):
Z-Average (d.nm): 21.12	Peak 1: 13.75	100.00	3.242
Pdl: 0.144	Peak 2: 0.000	0.0	0.000
Intercept: 0.917	Peak 3: 0.000	0.0	0.000
Result quality: Good			

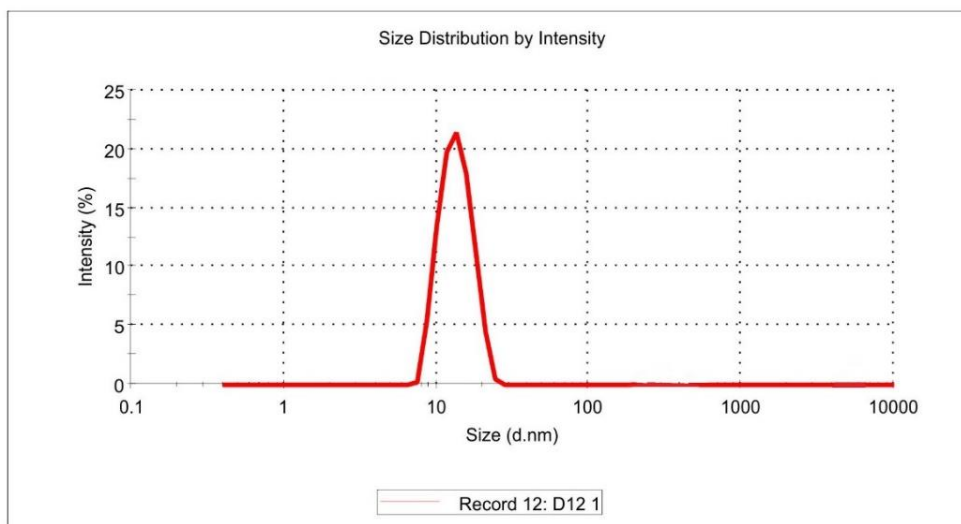


Figure 5.15: Globule size of optimized batch of AM-SMEDDS

5.11.2 Zeta potential determination

The zeta potential measurement is a crucial parameter which is highly useful for the assessment of the physical stability of colloidal dispersions. The zeta potential indicates the degree of repulsion between adjacent, similarly charged particles in dispersion. A high zeta potential value avoids the attraction forces and resists particle aggregation (14). Here, the zeta potential of the optimized batch was found to be -19.3 ± 1.8 mV (Figure 5.16). This indicates that the formulation is negatively charged owing to presence of free fatty acids of oil and repulsive forces predominates which makes the system stable by resisting aggregation of emulsion droplets (39).

Results

	Mean (mV)	Area (%)	Width (mV)
Zeta Potential (mV): -19.3	Peak 1: -19.3	100.0	9.79
Zeta Deviation (mV): 10.4	Peak 2: 0.0	0.0	0.00
Conductivity (mS/cm): 0.252	Peak 3: 0.00	0.0	0.00

Result quality : See result quality report

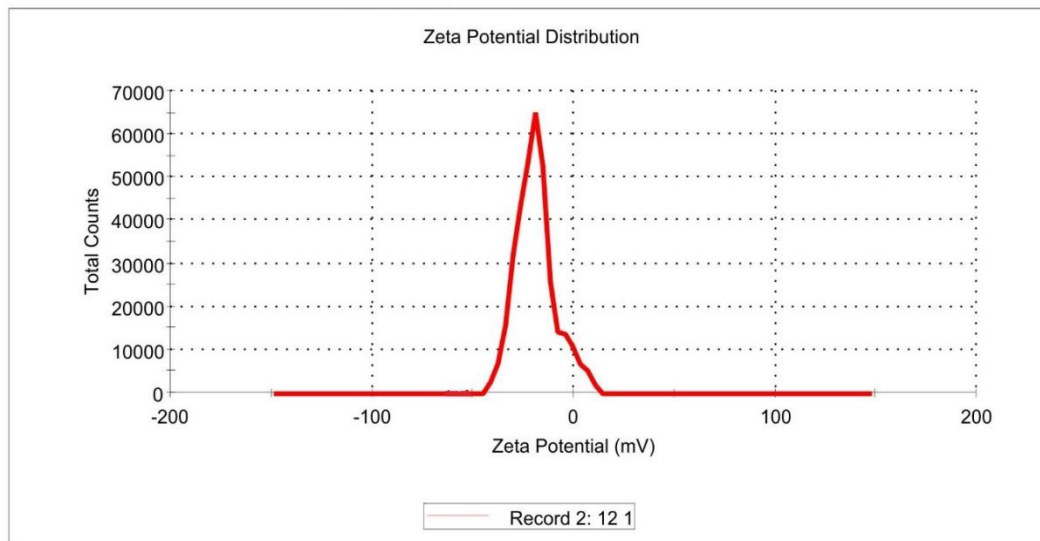


Figure 5.16: Zeta potential of optimized batch of AM-SMEDDS

5.11.3 Robustness to dilution

It is important to evaluate robustness to dilution of SMEDDS with different biological media because drug may precipitate at higher dilution in vivo and affect its absorption and permeation significantly. The formulation gets diluted at different extent with different media when administered orally. So, to mimic in vivo conditions, SMEDDS were diluted 50, 100, 250, 500 and 1000 times with different media. The globule size at all dilution was found to be less than 40 nm (Table 5.10). Results revealed that diluted SMEDDS did not show any precipitation or phase separation on storage in various dilution media. This confirms that the prepared SMEDDS were robust to dilution in all types of media. Furthermore, it also points out to the probability of uniform in vivo drug release profile when the formulation encounters gradual dilution (39).

Table 5.10: Robustness to dilution of AM-SMEDDS with different media

Media	50 times (nm)*	100 times (nm)*	250 times (nm)*	500 times (nm)*	1000 (nm)*
Distilled water	21.1±2.4	20.4±1.5	20.2±1.1	19.3±1.6	18.9±3.4
pH1.2	22.3±1.8	21.5±2.3	21.3±2.1	20.9±1.7	17.1±1.5
pH 6.8	24.8±2.1	22.3±2.8	23.3±2.5	21.9±3.1	21.3±1.9

*Data are presented as mean±SD, n=3.

5.11.4 Determination of self-emulsification time

The rate of emulsification was a major index for assessment of the efficiency of self-emulsification. The SMEDDS should disperse completely and quickly when subjected to dilution under mild agitation provided by GIT. Self-emulsification property of SMEDDS was identified visually by formulation of clear and stable monophasic liquid when diluting with aqueous media (40). The self-emulsification time of optimized batch was found to be 28±4 sec which indicated spontaneous formation of emulsion upon dilution with media which is a prerequisite of SMEDDS formulation.

5.11.5 Cloud Point determination

The cloud point is a crucial factor in SMEDDS particularly consisting of non-ionic surfactants as at temperature above cloud point, the formulation turns cloudy. Even at temperatures higher than the cloud point, dehydration of polyethylene oxide moiety of the non-ionic surfactant may occur resulting in phase separation, thereby affecting drug absorption (27,40). Hence, to circumvent these issues, the cloud point of the formulation should be over 37 °C. The developed AM-SMEDDS showed cloud point at 87 °C, indicating stability at physiological temperature encountered in GIT and also during storage (25).

5.11.6 Drug content determination

The drug content of optimized batch was found to be 99.8±1.69% suggesting uniform dispersion of drug in the formulation.

5.11.7 Viscosity determination

The viscosity of optimized batch was found to be 48.6±1.1 cP. The low value of viscosity is attributed to presence of less viscous Capryol 90 and Transcutol HP.

5.11.8 % Transmittance

% Transmittance of the optimized batch was found to be $99.2 \pm 0.4\%$ indicating formation of clear microemulsion upon dilution with aqueous media. The value closer to 100% indicated that the formulation was isotropic in nature. Here, the higher transmittance was attributed to low amount of oil and higher amount of surfactant (14).

5.11.9 Thermodynamic stability

The objective of thermodynamic stability study was to evaluate the phase separation and effect of temperature variation on developed SMEDDS in order to exclude the possibility of metastable formulations. If the SMEDDS formulations are stable in these conditions (heating cooling cycle and centrifugation), metastable formulation thus can be avoided and frequent tests need not be performed during storage. No signs of phase separation or precipitation was observed during heating/cooling cycle and centrifugation tests, indicating excellent stability of optimized batch of AM-loaded SMEDDS (23).

5.11.10 Fourier transform infrared spectroscopy (FTIR)

The IR spectra of AM, Capryol 90, physical mixture of drug and excipients and AM-SMEDDS are shown in figure 5.17. The FTIR spectra of AM showed characteristic peaks at 1612.49 cm^{-1} , 1442.75 cm^{-1} , 1091.71 cm^{-1} , 866.04 cm^{-1} indicative of C=C stretching, O-H bending, C-N stretching and C-Cl stretching respectively. The physical mixture of excipients showed characteristic peaks of all functional groups of drug and excipients. No additional peak was observed indicating compatibility between drug and excipients. FTIR spectra of AM-SMEDDS showed absence of characteristic peaks of AM indicating that drug was completely solubilized in oil phase of SMEDDS.

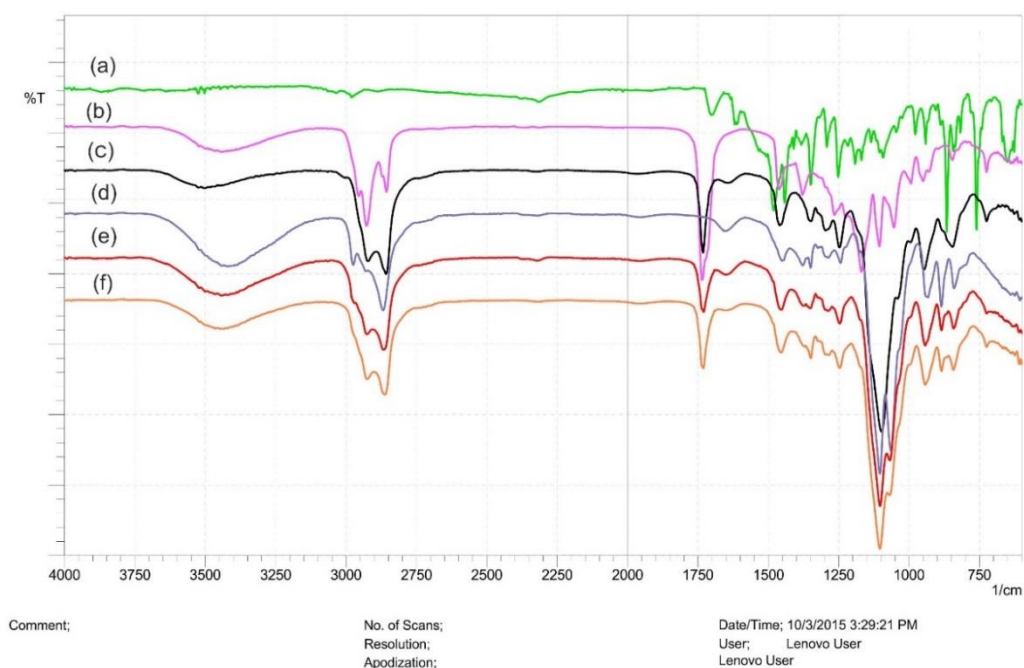


Figure 5.17 : FTIR spectrum of (a) AM (b) Capryol 90 (c) Cremophor EL (d) Transcutol HP (e) Physical mixture of AM and excipients (f) AM-SMEDDS

5.11.11 Transmission Electron Microscopy (TEM)

The TEM image of optimized batch showed spherical globules with globule size in the range of 20-40 nm which is in accordance with result obtained with zetasizer (Figure 5.18). Each globule was surrounded by thick layer indicating presence of surfactant layer. No sign of drug precipitation was observed inferring the stability of formulation.

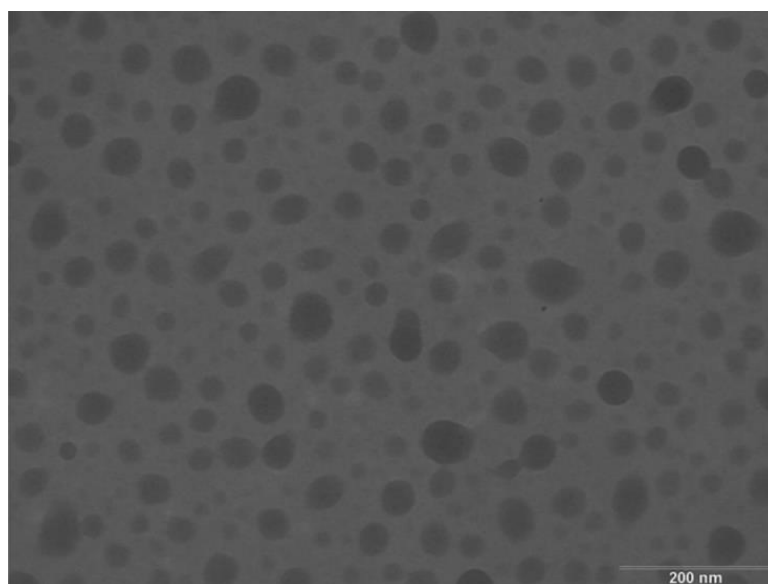


Figure 5.18: TEM image of optimized batch of AM-SMEDDS

5.12 IN VITRO DRUG RELEASE STUDY

The drug release profile of AM-SMEDDS and AM suspension is shown figure 5.19. In case of AM suspension, a fast release ($89.44 \pm 3.03\%$) of drug was observed in 2 h in acidic condition. Subsequent release of the drug in pH 6.8 was relatively slower and total $93.7 \pm 2.40\%$ of drug was released at the end of 8 hr.

In contrast for AM-SMEDDS, only $20.23 \pm 4.02\%$ of AM was released in acidic medium whereas more than $99.2 \pm 3.36\%$ of AM was released at the end of 8 hrs in phosphate buffer pH 6.8. Such slow release of AM from SMEDDS formulation owing to good affinity of AM for the oil phase (Capryol 90) indicates that a significant amount of drug will be carried to intestine inside the small microemulsion globules (41-43) which in turn will help in enhancing oral bioavailability via lymphatic uptake. The small globule size will provide high surface area, which will permit fast drug release.

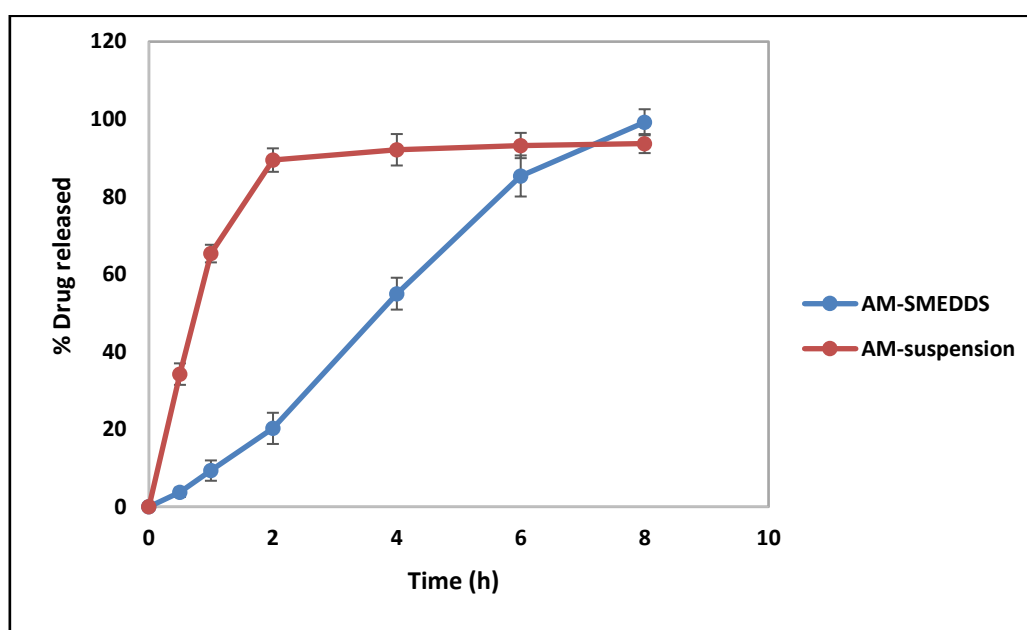


Figure 5.19 : In-vitro drug release profile of AM-SMEDDS and AM suspension

5.13 EX VIVO PERMEATION STUDY

Permeability in gastro intestinal tract of any formulation is a crucial factor which decides absorption and bioavailability of drug from that formulation. Hence ex vivo permeability studies were carried out to determine permeability of AM in stomach and intestine from SMEDDS and plain drug suspension. The release profile of AM suspension indicated most of the drug was permeated through stomach ($\sim 90\%$) and drug available for lymphatic uptake is very low.

In contrast, AM-SMEDDS showed only 15% diffusion through stomach and ~85% drug was diffused through intestinal membrane (Figure 5.20). Hence, it can be said that significant amount of drug will be carried to the intestine. Moreover, it can be assumed that the characteristics of microemulsion, such as nano-sized droplet size and the interaction between the surfactants (Cremophor EL, Transcutol HP) and intestinal membrane, may result in enhanced permeation of AM. Hence, it can be noted that permeation of the drug from the intestine was enhanced with SMEDDS, which fulfilled our objective of increasing intestinal permeability for enhancing the bioavailability of AM (23).

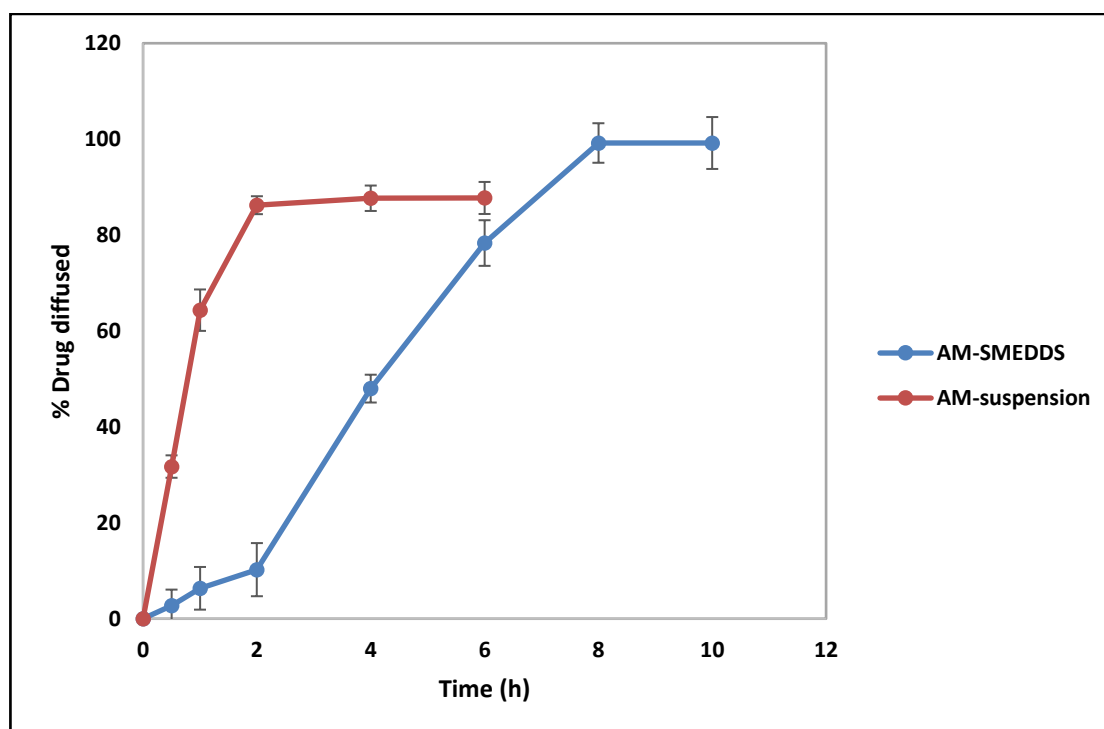


Figure 5.20: Ex vivo permeation study of AM-SMEDDS and AM suspension

5.14 STABILITY STUDY

The stability of AM loaded SMEDDS was monitored for 3 months at RT in terms of globule size, zeta potential, drug content and self-emulsification time. No significant change in the physicochemical parameters was observed during 3 months of storage at room temperature (Table 5.11).

Table 5.11: Characteristics of AM-SMEDDS after 3-months stability studies at different conditions

Time (months)	Room temperature ($30 \pm 2^\circ\text{C}/60\% \pm 5\% \text{RH}$)			
	Globule size* (nm)	Zeta potential (mV)	Drug content (%)	Self-emulsification time (min)
Initial	21.1±2.9	-19.3±1.8	99.8±1.7	28.0± 2.0
1 month	21.5±3.3	-19.1±2.8	99.1±2.2	28.0± 3.5
2 months	22.7±4.1	-18.7±4.7	98.4±3.3	30.5± 1.5
3 months	23.2±2.6	-17.5±3.9	98.1±1.8	32.0± 3.0

5.15 REFERENCES

1. Kohli K, Chopra S, Dhar D, S Arora S, Khar RK. self-emulsifying drug delivery system: An approach to enhance oral bioavailability. *Drug Discov Today*. 2010;15(21/22):958-965.
2. Gursoy RN, Benita S. Self-emulsifying drug delivery systems (SEDDS) for improved oral delivery of lipophilic drugs. *Biomed Pharmacother*. 2004;58:173–182.
3. Yeom DW, Song YS, Kim SR, Lee SG, Kang MH, Sangkil Lee S, Choi YW. Development and optimization of a self-microemulsifying drug delivery system for atorvastatin calcium by using d-optimal mixture design. *Int J Nanomedicine*. 2015;10:3865–3878.
4. Singh B, Singh R, Bandyopadhyay S, Kapil R, Garg B. Optimized nanoemulsifying systems with enhanced bioavailability of carvedilol. *Colloids Surf B*. 2013;101:465– 474.
5. Prajapati ST, Joshi H, Patel CN. Preparation and Characterization of Self Microemulsifying Drug Delivery System of Olmesartan Medoxomil for Bioavailability Improvement. *J Pharm*. 2013:1-9.
6. Singh S, Pathak K, Bali V. Product Development Studies on Surface-Adsorbed Nanoemulsion of Olmesartan Medoxomil as a Capsular Dosage Form. *AAPS PharmSciTech*. 2012;13(4):1212-1221.
7. Hua X, Lin C, Chen D, Zhang J, Liu Z, Wub W, Song H. Sirolimus solid self-microemulsifying pellets: Formulation development, characterization and bioavailability evaluation. *Int J Pharm*. 2012;438:123– 133.
8. Patel MR, Patel MH, Patel RB. Preparation and in vitro/ex vivo evaluation of nanoemulsion for transnasal delivery of paliperidone. *Applied Nanosci*. 2016;6(8):1095–1104.
9. Singh AK, Chaurasiya A, Singh M, Upadhyay SC, Mukherjee R, Khar RK. Exemestane Loaded Self-Microemulsifying Drug Delivery System (SMEDDS): Development and Optimization. *AAPS PharmSciTech*. 2008;9(2):628–634.
10. Holm R, Sonnergaard IHM. Optimization of Self-Microemulsifying Drug Delivery Systems (SMEDDS) Using a D-Optimal Design and the Desirability Function. *Drug Dev Ind Pharm*. 2006;32:1025–1032.

11. Balakumar K, Raghavan CV, selvana NT, Hari prasad R, Abdu S. Self nanoemulsifying drug delivery system (SNEDDS) of Rosuvastatin calcium: Design, formulation, bioavailability and pharmacokinetic evaluation. *Colloids Surf B*. 2013;112:337–343.
12. Shen H, Zhong M. Preparation and evaluation of self-microemulsifying drug delivery systems (SMEDDS) containing atorvastatin. *J Pharm Pharmacol*. 2006;58:1183–1191.
13. Beg S, Jena SS, Patra CN, Rizwan M, Swain S, Sruti J, Rao MEB, Singh B. Development of solid self-nanoemulsifying granules (SSNEGs) of ondansetron hydrochloride with enhanced bioavailability potential. *Colloids Surf B*. 2013;101 414– 423.
14. Parmar N, Singla N, Amin S, Kohli K. Study of cosurfactant effect on nanoemulsifying area and development of lercanidipine loaded (SNEDDS) self nanoemulsifying drug delivery system. *Colloids Surf B*. 2011;86:327–338.
15. Patel J, Dhingani A, Garala K, Raval M, Sheth N. Quality by design approach for oral bioavailability enhancement of Irbesartan by self-nanoemulsifying tablets. *Drug Deliv*. 2014;21(6):412-435.
16. Bandyopadhyay S, Katare OP, Singh B. Optimized self nano-emulsifying systems of ezetimibe with enhanced bioavailability potential using long chain and medium chain triglycerides. *Colloids Surf B*. 2012;100:50– 61.
17. Wu W, Wang Y, Que L. Enhanced bioavailability of silymarin by self-microemulsifying drug delivery system. *Eur J Pharm Biopharm*. 2006;63:288–294.
18. Seo YG, Kim DH, Ramasamy T, Kim JH, Marasini N, Oh YK, Kim DW, Kim JK, Yong CS, Kim JO, Choi HG. Development of docetaxel-loaded solid self-nanoemulsifying drug delivery system (SNEDDS) for enhanced chemotherapeutic effect. *Int J Pharm*. 2013;452:412– 420.
19. Shafiq S, Shakeel F, Talegaonkar S, Ahmad FJ, Khar RK, Ali M. Development and bioavailability assessment of ramipril nanoemulsion formulation. *Eur J Pharm Biopharm*. 2007;66 227–243.
20. Nepal PR, Han HK, Choi HK. Preparation and in vitro–in vivo evaluation of Witepsol® H35 based self-nanoemulsifying drug delivery systems (SNEDDS) of coenzyme Q10. *Eur J Pharm Sci*. 2010;39:224–232.

21. Gursoy RN, Benita S. Self-emulsifying drug delivery systems (SEDDS) for improved oral delivery of lipophilic drugs. *Biomed Pharmacother.* 2004;58:173–182.
22. El-Laithy HM, Basalious EB, El-Hosiny BM, Adel MM. Novel self-nanoemulsifying self-nanosuspension (SNESNS) for enhancing oral bioavailability of diacerein: Simultaneous portal blood absorption and lymphatic delivery. *Int J Pharm.* 2015;490(1-2):146-154.
23. Avachat AM, Patel VG. Self nanoemulsifying drug delivery system of stabilized ellagic acid–phospholipid complex with improved dissolution and permeability. *Saudi Pharm J.* 2015;23(3):276-289.
24. Pouton CW. Formulation of poorly water-soluble drugs for oral administration: physicochemical and physiological issues and the lipid formulation classification system. *Eur J Pharm Sci.* 2006;29:278–287.
25. Wang L, Dong J, Chen J, Eastoe J, Li X. Design and optimization of new self-nanoemulsifying drug delivery system. *J Colloid Interface Sci.* 2009;330:443–448.
26. Dash RN, Habibuddin M, Humaira T, Ramesh D. Design, optimization and evaluation of glipizide solid self-nanoemulsifying drug delivery for enhanced solubility and dissolution *Saudi Pharm J.* 2015;23(5):528-540.
27. Bandyopadhyay S, Katare OP, Singh B. Optimized self nano-emulsifying systems of ezetimibe with enhanced bioavailability potential using long chain and medium chain triglycerides. *Colloids Surf B.* 2012;100:50– 61.
28. Pouton CW, Porter CJ. Formulation of lipid-based delivery systems for oral administration: materials, methods and strategies. *Adv Drug Deliv Rev.* 2008;60(6):625-37.
29. Rao SVR, Shao J. 2008. Self-nanoemulsifying drug delivery systems (SNEDDS) for oral delivery of protein drugs. I. Formulation development. *Int J Pharm.* 2008;362:2–9.
30. Craig D, Barker S, Banning D, Booth S. An investigation into the mechanisms of self-emulsification using particle size analysis and low frequency dielectric spectroscopy. *Int J Pharm.* 1995;114:103–110.
31. Pouton CW. Formulation of self-emulsifying drug delivery systems. *Adv Drug Deliv Rev.* 1997;25:47–58.

32. Kallakunta VR, Bandari S, Jukanti R, Veerareddy PR. Oral self emulsifying powder of lercanidipine hydrochloride: Formulation and evaluation. *Powder Technol.* 2012;221:375–382.
33. McConville C, Friend D. Development and characterisation of a self-microemulsifying drug delivery systems (SMEDDSs) for the vaginal administration of the antiretroviral UC-781. *Eur J Pharm Biopharm.* 2013;83:322–329.
34. Lee DW, Marasini N, Poudel BK, Kim JH, Cho HJ, Moon BK, Choi HG, Yong CS, Kim JO. Application of Box–Behnken design in the preparation and optimization of fenofibrate-loaded self-microemulsifying drug delivery system (SMEDDS). *J Microencapsul.* 2014;31(1):31–40.
35. Bahloul B, Lassoued MA, Sfar S. A novel approach for the development and optimization of selfifying drug delivery system using HLB and response surface methodology: Application to fenofibrate encapsulation. *Int J Pharm.* 2014;466:341–348
36. Beg S, Sandhu PS, Batra RS, Khurana RK, Singh B. QbD-based systematic development of novel optimized solid self-nanoemulsifying drug delivery systems (SNEDDS) of lovastatin with enhanced biopharmaceutical performance. *Drug Deliv.* 2015;22(6):765-784.
37. Balakrishnan P, Lee BJ, Oh DH, Kim JO, Hong MJ, Jee MP, Kim JA, Yoo BK, Woo JS Yong CS, Choi HG. Enhanced oral bioavailability of dexibuprofen by a novel solid Self-emulsifying drug delivery system (SEDDS). *Eur J Pharm Biopharm.* 2009;72:539–545.
38. Elnaggar YS, El-Massik MA, Abdallah OY. Self-nanoemulsifying drug delivery systems of tamoxifen citrate: design and optimization. *Int J Pharm.* 2009;380(1-2):133-141.
39. Kamel R, Basha M. Preparation and in vitro evaluation of rutin nanostructured liquisolid delivery system. *Bulletin Faculty Pharm.* 2013;51:261–272.
40. Itoh K, Tozuka Y, Oguchi T, Yamamoto K. Improvement of physicochemical properties of N-4472 part I formulation design by using self-microemulsifying system. *Int J Pharm.* 2002;238:153–160.
41. Zhang P, Liu Y, Feng N, Xu J. Preparation and evaluation of self microemulsifying drug delivery system of oridonin. *Int J Pharm.* 2008;355:269–276.